Review Article

Multimodal imaging for radiation therapy planning in patients with primary prostate cancer

Constantinos Zamboglou[a,h,i,*], Matthias Eiber[b,h], Thomas R. Fassbender[c], Matthias Eder[c], Simon Kirste[a,h], Michael Bock[d,h], Oliver Schilling[e,h], Kathrin Reichel[f], Uulke A. van der Heide[g], Anca L. Grosu[a,h]

[a] Department of Radiation Oncology, Medical Center – University of Freiburg, Faculty of Medicine, University of Freiburg, Germany
[b] Department of Nuclear Medicine, Klinikum rechts der Isar, Technical University Munich, Germany
[c] Department of Nuclear Medicine, Medical Center – University of Freiburg, Faculty of Medicine, University of Freiburg, Germany
[d] Division of Medical Physics, Department of Radiology, Medical Center – University of Freiburg, Faculty of Medicine, University of Freiburg, Germany
[e] Institute of Surgical Pathology, Medical Center – University of Freiburg, Faculty of Medicine, University of Freiburg, Germany
[f] Department of Urology, Medical Center – University of Freiburg, Faculty of Medicine, University of Freiburg, Germany
[g] Department of Radiation Oncology, The Netherlands Cancer Institute, Amsterdam, the Netherlands
[h] German Cancer Consortium (DKTK), Partner Site Freiburg, Germany
[i] Berta-Ottenstein-Programme, Faculty of Medicine, University of Freiburg, Germany

A B S T R A C T

Implementation of advanced imaging techniques like multiparametric magnetic resonance imaging (mpMRI) or Positron Emission Tomography (PET) in radiation therapy (RT) planning of patients with primary prostate cancer demands several preconditions: accurate staging of the extraprostatic and intraprostatic tumor mass, robust delineation of the intraprostatic gross tumor volume (GTV) and a reproducible characterization of the prostate cancer's biological properties. In the current review we searched for the currently available imaging techniques and we discussed their ability to fulfill these preconditions.

We found that current pretreatment imaging was mainly performed with mpMRI and/or Prostate-specific membrane antigen PET imaging. Both techniques offered an accurate detection of the extraprostatic and intraprostatic tumor burden and had a major impact on RT concepts. However, some studies postulated that mpMRI and PSMA PET had complementary information for intraprostatic GTV detection. Moreover, interobserver differences for intraprostatic tumor delineation based on mpMRI were observed. It is currently unclear whether PET based GTV delineation underlies also interobserver heterogeneity. Further research is warranted to answer whether multimodal imaging is able to visualize biological processes related to prostate cancer pathophysiology and radiation resistance.

1. Introduction

In the last decade, improvement in advanced medical imaging techniques such as multiparametric magnetic resonance imaging (mpMRI) or Positron Emission Tomography (PET) enabled the depiction of anatomic and functional properties of intraprostatic lesions, lymph node metastases and distant metastases in patients with primary prostate cancer (PCa). However, the implementation of these techniques in radiation therapy (RT) planning for primary PCa progresses only slowly.

Current guidelines for patients with primary PCa [1] recommend a risk-adapted **staging** procedure taking into account the patients' preference and comorbidity. MpMRI should be used for local staging in patients with intermediate- and high-risk PCa, whilst at least cross-sectional abdominopelvic imaging and bone scan are recommended for metastatic screening.

In patients with primary PCa conventional RT techniques aim at delivering a homogeneous dose to the entire prostatic gland without considering the localization of imaging defined intraprostatic tumour mass. Evidence from PCa dose-escalation studies suggests an improved tumour control based on this RT dose increase [2–4]. However, an unlimited dose escalation to the whole prostatic gland is limited by radiation damage occurring to neighboring organs at risk [5]. Likewise, strategies to escalate the RT dose to the gross tumor volume (GTV) within the prostate have been proposed [6]. One major issue for every single **focal therapy** regimen is the accurate detection and delineation of the GTV by implementation of the appropriate imaging technique. Most of the studies used mpMRI to guide focal RT dose escalation by external beam RT (EBRT) or brachytherapy (high-dose or low-dose rate BT) [6]. Current advances in PET imaging showed very encouraging results in identifying the GTV within the prostate [7–9] and some studies postulated that the combined use of mpMRI and PET information

achieves the best results in GTV detection and delineation [7,10].

For patients with primary PCa **risk stratification** is mandatory to select suitable treatment options. The National Comprehensive Cancer Network (NCCN; available from: www.nccn.org) risk-classification system implements clinical T stage (cT stage), Gleason score, and initial prostate-specific antigen (iPSA) levels. All of them have been shown to be independent risk factors of biochemical failure (BF) after definitive RT [11]. However, predicting the final outcome through models can be impeded due to patient heterogeneity [12], making detection of more robust risk-factors a necessity. In current practice, features from modern imaging data have impact on cT stage by defining the tumour localization. However, first studies postulated that features extracted from MRI [13,14] or PET [15] data may help to characterize the intraprostatic GTV in terms of biological aggressiveness, improving patients' risk stratification. Imaging features allow non-invasive PCa characterization, enabled through longitudinal observations at multiple time-points during treatment [16]. Adding to that, the implementation of modern imaging for GTV characterization may account for intratumoral heterogeneity in PCa [17].

Modern imaging techniques must fulfill several preconditions to support radiation oncologists in treatment planning: accurate staging of the extraprostatic and intraprostatic tumor mass, robust delineation of the intraprostatic GTV and a reproducible characterization of the PCa's biological properties. In this review we discussed whether the currently available imaging techniques, emphasizing on mpMRI and Prostate-specific membrane antigen (PSMA) PET, are able to fulfill these preconditions.

2. Materials and methods

A search of the PubMed database for the period from January 1, 2010 to July 30, 2018 was conducted. The following search strategy was applied "(imaging [tw] OR MRI[tw] OR magnetic resonance imaging[tw] OR PET[tw] OR positron emission tomography[tw]) AND prostate[tw] OR prostatic[tw])". Only papers reporting on treatment naïve patients were included. The included papers needed to be available as full published manuscripts and had to be written in English. Full text versions of the eligible papers were retrieved and reviewed including manual searching of the bibliographies for other applicable papers.

3. Results

3.1. Metastatic screening

The depiction of the systemic tumour burden is crucial, greatly affecting therapeutic decision and stratifies: local therapy (prostate and/or pelvic lymph nodes) versus oligometastatic directed therapy versus systemic therapy. The sensitivities and specificities for detecting extraprostatic PCa in multimodal imaging are summarized in Table 1.

3.1.1. MpMR

MpMRI for staging of patients with primary PCa normally consists of T1w and T2w imaging in combination with one or two additional methods such as diffusion (DWI) MRI or dynamic contrast enhanced (DCE) MRI. DWI depictures the membrane integrity and tissue cellularity and is quantified by the Apparent Diffusion Coefficient (ADC), representing the diffusion coefficient of water molecules in the tissue. DCE-MRI reflects the density and permeability of tumour infiltrating micro-vessels. Some studies used MR-spectroscopy as an additional part of mpMRI protocols. Staging of lymph node metastases in patients with primary PCa is still heavily relying on anatomical MRI sequences (T1w and T2w). However, malignant lymph nodes may be normal sized and non-metastatic lymph nodes may be enlarged due to reactive hyperplasia. Likewise, a meta-analysis reported a pooled sensitivity of 0.39 and a pooled specificity for 0.82 for MRI in lymph node staging [18]

using histology as the gold-standard. The addition of DWI-MRI may improve the sensitivity as well as the specificity for lymph node detection [19]. Harisinghani et al. showed that MRI with paramagnetic nanopartices improved the sensitivity from 0.35 to 0.91 compared to conventional MRI [20].

Staging of bone metastases with MRI can be done either by whole-body MRI or by axial skeleton images and is mainly performed with T1w or DWI [21]. A recent meta-analysis by Who et al. [21] included ten studies that used MRI for the detection of bone metastasis in patients with PCa showing a pooled sensitivity of 0.96 and a specificity 0.98. Lecouvet et al. compared MRI with bone scintigraphy in 66 patients with high-risk PCa and reported a change in treatment plan in 22% of the patients due to MR findings. The authors also analyzed the economic impact and observed variability among different countries with a trend for higher costs for MR imaging [22].

3.1.2. Psma Pet/Ct

PSMA is a type II membrane glycoprotein which is expressed at levels that are up to several thousand-fold in PCa tissue than in benign prostatic tissue. Salivary glands, kidneys and proximal small intestine exhibit high PSMA-expression which however does not impair image interpretation [23]. Additionally, PSMA expression may increase as tumor grade and castrate resistance increases [24]. It should be mentioned that Mannweiler et al. observed an inhomogeneous PSMA expression by immunostaining of primary PCa lesions identifying that, 6 from 51 intraprostatic lesions had no to low PSMA expression [25]. Today, mainly small molecule PSMA ligands with urea-based binding motif are labeled with ^{68}Ga- or ^{18}F- for clinical practice [8,15,26–31].

First studies analyzed the value of PSMA PET/CT in detection of lymph nodes metastases in patients with primary PCa [32,33]. Maurer et al. compared the performance of ^{68}Ga-PSMA-11 PET/CT for lymph node detection with conventional cross sectional imaging using histopathological evaluation as the reference and reported sensitivities 0.66 and 0.44 and specificities of 0.99 and 0.85 for PSMA PET and conventional imaging, respectively. Furthermore, the authors could show that even lesions with 2 mm can be detected with PSMA PET [34]. Leeuwen et al. observed a similar sensitivity (0.64) and specificity (0.95) for lymph node detection by comparing ^{68}Ga-PSMA-11 PET/CT with histology reference [35]. Using also histology as the reference Öbek et al. reported lower sensitivity (0.54) and specificity (0.86) for ^{68}Ga-PSMA-11 PET/CT [36]. Mix et al. performed ^{111}In-PSMA-617-guided lymphadenectomy with the use of a gamma probe. Ex situ analysis at the level of single lymph nodes revealed that ^{111}In-PSMA-617 had excellent ability to discriminate between malignant and non-malignant LN in six patients with PCa (sensitivity 0.92 and specificity 0.99) [37]. A recent study by Rischpler et al. identified PSMA uptake in ganglia as an important pitfall due to similar imaging characteristics with malignant lymph nodes [38].

For the detection of bone metastases, PSMA PET has a higher sensitivity (0.99 vs. 0.87) and specificity (0.88 vs. 0.61) [39] and detects on average double the number of lesions than standard bone scintigraphy [40]. However, a review by Sheikhbahaei et al. noted that due to pathological bone remodeling and increased vascularity false positive PSMA PET findings may occur in benign bone disease such as Paget's disease. Additionally, several case reports reported on the incidental detection of synchronous primary and metastatic lesions from other malignancies like multiple myeloma or tumors of the gastrointestinal tract [41].

A prospective multicenter study reported that ^{68}Ga-PSMA-11 PET/CT led to a change in management intend in 21% of the patients with primary [42]. Dewes et al. observed a change of overall RT concept in 33% of the patients with primary PCa using ^{68}Ga-PSMA-11 PET/CT. The authors performed additional RT of the pelvic lymph nodes in 25% of the patients due to findings in PSMA PET [43]. Schiller et al. delineated a clinical target volume according to the Radiation Therapy Oncology Group guidelines to cover the pelvic lymphatics in 25 patients

Table 1
Sensitivity and specificity for detection of lymph node and bone metastases.

Study	Patients	Technique	Sensitivity	Specificity
I Lymph node metastases				
Hovels et al. [18]	628 (meta-analysis)	MRI***	0.39	0.82
Harisinghani et al. [20]	80	MRI with paramagnetic nanoparticels	0.91	0.98
Vallini et al. [19]	26	DWI - MRI	0.85	0.9
Maurer et al. [34]	130	^{68}Ga-PSMA-11	0.66	0.99
Van Leuwen et al. [35]	30	^{68}Ga-PSMA-11	0.64	0.95
Öbek et al. [36]	51	^{68}Ga-PSMA-11	0.54	0.86
Jilg et al.* [106]	30	^{68}Ga-PSMA-11	0.81	1
*II Bone metastases***				
Study	Patients	Technique	Sensitivity	Specificity
Who et al. [21]	1031 (metaanalysis)	MRI***	0.96	0.98
Pyka et al. [39]	126	^{68}Ga-PSMA-11	0.99	0.88

Please note:
* The study by Jilg et al. was performed in patients with rising PSA after prostatectomy.
** No histology reference was used in the studies considering bone metastases.
*** MRI technique was not further specified.

with high-risk PCa who underwent ^{68}Ga-PSMA-11 PET/CT before RT. The authors observed that 35.7% of the PSMA PET positive lymph nodes were not covered by the RT field in these patients [44].

3.1.3. PET-tracers other than PSMA-ligands

Several PET tracers have been investigated for staging of patients with primary PCa. The most commonly used radiotracer for oncologic imaging is 2-deoxy-2-(^{18}F)fluoro-D-glucose (FDG) but it is of limited utility in PCa patients due to low glucose metabolism in PCa lesions [45,46]. PET/CT using [^{11}C]- and [^{18}F]-labelled choline derivates were widely used for staging of primary PCa [47]. However, a meta-analysis by Evangelista et al. [48] and a recent study by Selnaes et al. [49] reported for choline PET/CT and also for 18-F-Fluciclovine PET/CT a low sensitivity (< 0.5) in detection of metastases from primary PCa.

Mosavi et al. compared whole-body DWI- MRI with ^{18}F-NaF PET/CT for detection of bone metastases in patients with high-risk PCa reporting a higher sensitivity but a lower specificity for PET [50]. Neuroendocrine transformation occurs in advanced PCa and the usage of ^{68}Ga-DOTATOC PET examinations for characterization on neuroendocrine differentiation was proposed [51].

3.2. Detection, delineation and characterization of intraprostatic lesions

The implementation of modern imaging techniques for local staging of PCa should meet several preconditions:

High sensitivity and specificity in detection of intraprostatic GTV
Robust delineation of intraprostatic GTV
Characterization of the biological properties of intraprostatic GTV

3.2.1. MpMRI

MpMRI detects intraprostatic PCa with high accuracy if anatomical and functional MRI information is combined from T2w-, DCE- and DWI-MRI. Using the combination of all three sequences two meta-analyses reported pooled sensitivities and specificities as high as 74–89% and 73–88% for the detection of intraprostatic lesions (1.5 or 3 Tesla MRI systems) [52,53]. De Rooji et al. observed differences in pooled sensitivities and specificities between studies using prostatectomy (69% and 93%) or studies using biopsy (76% and 86%) as the reference standard [52].

MpMRI has poor sensitivity in small (< 0.5 ml) PCa lesions [54], low-grade PCa as well as T-zone involvement and suffers from false-positive rates in benign prostatic hyperplasia [55]. A confounding factor in tumor detection with mpMRI, is the presence of post-biopsy or post-fiducial marker insertion hematoma (especially in T2w and DCE) and changes induced by androgen deprivation therapy [56].

Furthermore, mpMR image interpretation for PCa diagnosis is reported to result in substantial inter-reader variability [57] which impacts intraprostatic tumour delineation [58,59]. In a study by Steenbergen et al. six teams of delineators contoured the intraprostatic tumour volume in 20 patients based on mpMRI information and used prostatectomy as the reference. The interobserver agreement between delineations of the teams and the pathologist was only moderate (kappa 0.45 ± 0.16) and one dominant lesion in the central zone was missed by all teams [58]. Rischke et al. could prove that a DWI-MRI based GTV-delineation resulted in higher intraobserver variability compared to DCE- or T2w-based approaches [60]. To standardize the evaluation and reporting of mpMRI of the prostate an updated version of the Prostate Imaging Reporting and Data System (PI-RADSv2) was released [61]. In the new PI-RADS v2 the dominant sequence to detect PCa in the peripheral zone is DWI. For PCa detection in the transition zone T2w is the most important sequence, whereas DCE-MRI has been attributed a minor role in both locations. A study by Venderink et al., defined intraprostatic lesions according to PI-RADSv2 and performed direct in-bore MRI-guided biopsies in patients with clinically suspicious PCa and detected increased PCa detection rates in patients with higher PI-RADv2 scores [62]. Furthermore, several studies discovered that patients with higher PI-RADSv2 lesions are more likely to have high-grade PCa (defined by Gleason score $\geq$ 7a (3 + 4)) [63,64]. Another approach to increase the robustness of mpMRI-based detection and delineation of intraprostatic tumour lesions is the implementation of computer-aided methods (CADs) [65]. Viswanath et al. observed that PCa lesions in the central gland and in the peripheral zone have significantly differing textural quantitative imaging signatures on T2w-MRI [66]. Several groups implemented algorithms with deep learning architecture to improve CAD in PCa detection [67,68]. Algohary et al. proposed that radiomic features extracted from T2- and ADC-MRI can distinguish between malignant and normal regions in the prostate (defined by biopsy) [69]. Wang et al. compared deep learning with deep convolutional neural network and a non-deep learning algorithm (SIFT image feature and bag-of-word) to distinguish pathologically confirmed PCa patients from non-malignant conditions and reported significant higher AUC values (0.84 vs 0.7) for the deep learning approach [70].

Notably, as mpMRI is not able to fully exhibit intraprostatic tumour amount it is still debated whether it is able to identify to most aggressive lesions. Three studies examined whether local recurrences of PCa after primary radiation therapy (RT) occur at the primary tumour side using pre and post treatment MRI in a limited number of patients. All of them observed that local recurrences after RT mostly occurred at the side of the primary MR-visible tumour [71–73]. Quivrin et al. retrospectively defined the intraprostatic GTV based on MRI in 66 PCa

patients treated with low-dose brachytherapy and showed that the dose distribution within the GTV had a predictive value on PSA bounce after brachytherapy [74]. Zamboglou et al. delineated retrospectively the intraprostatic GTV based on mpMRI in patients with primary EBRT for PCa. The study could show that the dose distribution within the imaging-defined GTV correlates better with the biochemical recurrent free survival than the RT dose delivered to the rest of the prostatic gland [75].

Therefore, the ability of mpMRI to characterize the aggressiveness of the intraprostatic GTV requires further investigation. An accurate and precise characterization of the GTV would improve the risk stratification of PCa patients and would allow for an individualization of RT procedures (e.g. dose de- and/or escalation in certain GTV sub-volumes according to imaging information). One important approach is the correlation of features extracted from imaging with parameters deduced from histology reference. Gibbs et al. reported a significant correlation between cell density and ADC values [76]. Donati et al. demonstrated that the ADCmean is an independent predictor of tumor aggressiveness in terms of Gleason score [13]. Likewise, Casares-Magaz et al. introduced a tumour control probability (TCP) model for RT of PCa using information from ADC [77]. Another approach is to correlate imaging derived features with the outcome after therapy. Two studies reported that the intraprostatic tumour extent and extracapsular disease defined by mpMRI correlates with the outcome after primary RT for prostate cancer [78,79]. Another study could prove that texture features (e.g. Haralick features) on T2w-MRI are associated with biochemical recurrence after RT for PCa [80]. Song et al. observed a significant increase of ADC values in PCa lesions during RT and proposed the usage of DWI MRI as a potential imaging biomarker for monitoring therapeutic response [81].

First prospective studies reported outcomes after mpMRI-guided focal RT for patients with primary PCa. A Spanish Phase II study performed RT dose escalation by MRI-transrectal ultrasound fusion HDR BT [82]. Dose escalation on intraprostatic GTV was feasible in 14/15 patients and with a median follow-up of 18 months no patient developed gastrointestinal/genitourinary toxicities ≥ 3. Recently, a randomized, multicenter Phase III study (FLAME trial) reported toxicity outcomes after a median follow-up of 55 month in 571 patients [83]. The standard treatment arm received a dose to the entire prostate of 77 Gy in 35 fractions. The dose-escalated treatment arm received 77 Gy in 35 fractions to the entire prostate, including an integrated boost up to 95 Gy to the MRI defined PCa. Prevalence rates for both gastrointestinal and genitourethral side effects were not significantly different across treatment groups. Additionally, several retrospective analyses underlined the feasibility of MRI-guided focal RT using stereotactic body RT, intensity modulated RT (IMRT) or BT [6].

3.2.2. psma pet/ct

Lopci et al. performed ^{68}Ga-PSMA-11 PET/CT in patients with previous negative mpMRI findings or contraindications for mpMRI imaging and intraprostatic PSMA uptake was found in 25 of 45 patients. However, PCa was found by PET guided fusion biopsy in 11 of these 25 patients [84]. Eight studies investigated the potential implication of

PSMA PET/CT in intraprostatic tumor localization using prostatectomy as the reference (Table 2). There is a broad heterogeneity with regard to data acquisition (e.g. registration techniques between histology and imaging information, included patient cohorts and the used PET tracer) and data analysis (e.g. level of correlation between imaging and histology information). The median sensitivities, specificities and ROC-AUC values for all studies were 0.71 (range: 0.49–0.92), 0.92 (range: 81–97) and 0.83 (range: 0.83–0.84), respectively.

In the studies mentioned in table 2 the detection and delineation of intraprostatic GTVs was mainly performed manually by experienced readers. In a voxel-level correlation between PSMA PET and histology using receiver operating characteristic (ROC) analyses a threshold of 30% of SUVmax within the prostate for GTV-delineation is useful to reach a sensitivity ≥ 0.9 [8]. Two other studies used different thresholds for PSMA-based GTV-delineation (40% and 50% of SUVmax within the prostate), respectively [85,86]. To the best of our knowledge no interobserver variation analysis for PSMA PET based GTV-delineation in the prostate was performed until now. Furthermore, no CAD approach was introduced for PSMA PET based PCa detection or delineation.

The correlation of PSMA PET signal with the Gleason score is currently debatable. A recent work by Bravaccini et al. found a strong correlation between PSMA signal (immunohistochemistry) in biopsy cores and prostatectomy specimen with the corresponding Gleason scores and PSA serum levels. In Gleason pattern 3 vs. Gleason pattern 4 and 5, PSMA sensitivity and specificity were 0.84 and 0.95 [87]. Hoffmann et al. compared ^{68}Ga-PSMA-11 PET signal with Gleason score in biopsy cores derived from TRUS-guided biopsies and reported that the PSMA signal allows to distinguish between Gleason score 7a and 7b tumours [88]. This observation was supported by Rhee et al. using prostatectomy as the reference [30]. Rowe et al. used prostatectomy as the reference and detected a positive correlation between ^{18}F-DCFBC uptake in tumors with Gleason score ($\rho > 0.65$ and $p < 0.05$) [15]. On the contrary, three studies using prostatectomy as the reference did not observed a significant correlation between ^{68}Ga-PSMA-11 PSMA signal and Gleason score [8,27,28].

There is lack in clinical experience regarding PSMA PET-guided focal RT (Fig. 2). However, Zamboglou et al. performed an IMRT planning study simulating a dose escalation on PSMA PET derived targets while calculating the tumor control probability based on the dose distribution within the registered histological information (TCP-histo). We could demonstrate that PSMA PET guided RT dose escalation considering the FLAME trial protocol [89] was feasible in ten of ten patients. Furthermore, TCP-histo was significant higher in the dose escalation arm compared to the conventionally fractionated arm (70% vs. 96%, $p < 0.01$) without increased risk of normal tissue toxicity [90].

3.2.3. Combined use of PSMA PET and mpMRI

Combing information from mpMRI and PSMA PET might offer complementary information in PCa detection overcoming the limitation of each single technique to identify the entire intraprostatic tumour amount. In a first study by Zamboglou et al. the authors compared

Table 2
Correlation studies between PSMA PET and histopathology after radical prostatectomy.

| Study	Patients	Tracer	Registration PET vs histology	Analysis	Sensitivity	Specificity	ROC-AUC
Fendler et al. [26]	21	^{68}Ga-PSMA-11	no	6 segments	0.67	0.97	0.84
Eiber et al. [27]	53	^{68}Ga-PSMA-11	no	6 segments	0.64	0.94	0.83
Rahbar et al. [28]	6	^{68}Ga-PSMA-11	No	22 segments	0.92	0.92	
Zamboglou et al. [29]	11	^{68}Ga-PSMA-11	Ex-vivo CT, manual registration	48 segments	0.75	0.87	
Zamboglou et al. [8]	9	^{68}Ga-PSMA-11	Ex-vivo CT, multiple registration steps	Voxel-level			0.83
Rhee et al. [30]	20	^{68}Ga-PSMA-11	Deformable registration	27 segments	0.49	0.95	
Berger et al. [112]	50	^{68}Ga-PSMA-11	no	8 segments	0.81	0.85	
Kesch et al. [31]	10	^{18}F-PSMA-1007	no	38 segments	0.71	0.81	
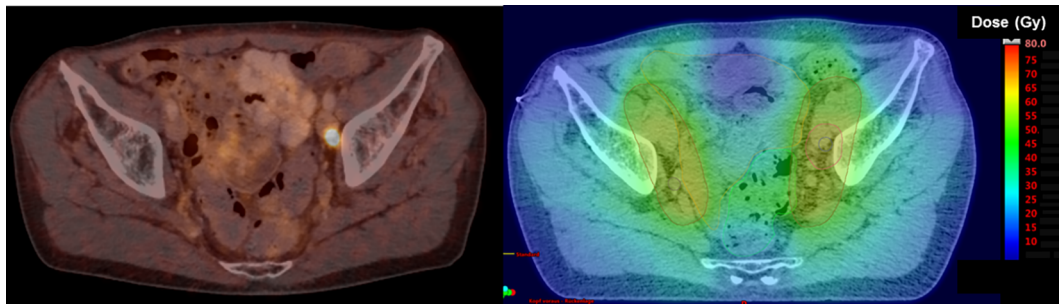
Fig. 1. A clinical example of PSMA PET guided IMRT in a patient with positive lymph nodes. A 74 year old patient presented with primary PCa: Gleason 9 (4 + 5), initial PSA 15 ng/ml and cT3b stadium. The patient had 60% chance for lymph node involvement according to MSKCC nomogram. PSMA PET/CT revealed one lymph node in the left (left picture) and one lymph node in the right pelvis (not shown). The patient had neoadjuvant ADT in combination with IMRT and IGRT: 76 Gy to the prostate, 45 Gy to the pelvic lymph nodes and a sequential boost to the 2 PET positive lymph nodes with up to 54 Gy. In the right picture the dose wash representation of the IMRT plan is shown.

mpMRI and ^{68}Ga-PSMA-11 for intraprostatic GTV-delineation and we found only 40% overlap between GTV-MRI and GTV-PET. Furthermore, the laterality on mpMRI, PSMA PET and histopathology after TRUS-biopsy was similar in only 47% of the patients. The GTVs based on PSMA PET were significantly larger than the GTVs based on mpMRI [91]. Tulsyan et al. compared ^{68}Ga-PSMA-11 with mpMRI for staging of high-risk PCa patients and observed similar results (concordance in 52.7% of patients) [92]. In contrast Giesel et al. reported a high concordance in tumour extension between PSMA PET (delineated by 50% of SUVmax) and mpMRI (T2w and DWI) [85]. Table 3 summarizes studies which performed intra-individual comparisons between PSMA PET/CT, mpMRI and histopathology after prostatectomy using again different approaches not only in data acquisition, but also in data analysis. For all studies the median sensitivities/specificities for PSMA PET and mpMRI were 0.71 (range: 0.49–0.75)/0.87 (range: 0.81–0.95) and 0.65 (range: 0.43–0.86)/0.82 (range: 0.64–0.94), respectively.

Thalgott et al. compared Ga-PSMA-11 PET/MRI findings to pre-operative staging nomograms in PCa patients using histopathology as the reference [93]. Considering extracapsular disease and seminal vesicle invasion combined PET/MR imaging yielded the highest

Table 3
Correlation studies between PSMA PET, mpMRI and histopathology after radical prostatectomy.

Study	PSMA PET		mpMRI	
	Sensitivity	Specificity	Sensitivity	Specificity
Eiber et al. [27]	0.64	0.94	0.43–0.58[*]	0.82–98[*]
Zamboglou et al. [29]	0.75	0.87	0.7	0.82
Rhee et al. [30]	0.49	0.95	0.44	0.94
Berger et al. [112]	0.81	0.85	0.65	0.83
Kesch et al. [31]	0.71	0.81	0.86	0.64

 * Different Youden thresholds were used for analysis. All studies used an mpMRI protocol including: T2w-, DCE-, and DWI-MRI.

sensitivity compared to the MSKCC nomogram and the Partin tables.

Using hybrid PET/MR Eiber et al. indicated, that mpMRI and ^{68}Ga-PSMA-11 PSMA may offer complementary information in PCa detection. The sensitivity increased to 0.76 when both imaging methods were combined. The authors divided the prostate into sextants and observed
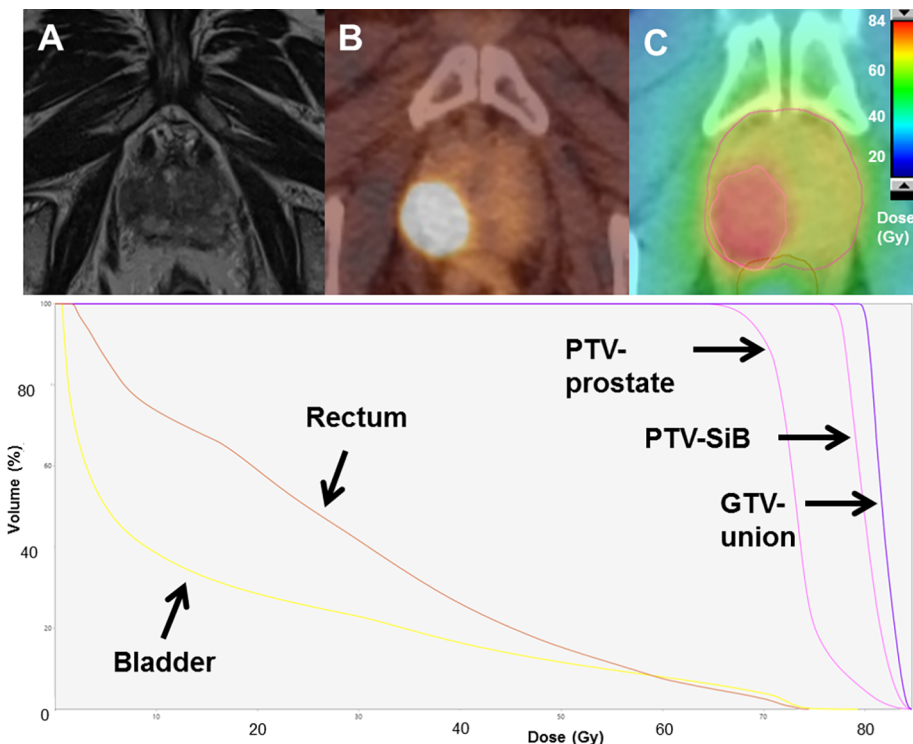

Fig. 2. A clinical example for IMRT dose escalation on multimodal defined intraprostatic lesions. In A and B axialT2-MRI and PSMA PET images are shown with PCa in the right lobe of a 72 year old patient with intermediate risk PCa according to NCCN. The patient received PSMA planning PET/CT and mpMRI imaging after insertion of fiducial markers. Using image-guided RT (IGRT) and IMRT (rapid-arc) we delivered 74 Gy (1.85 Gy per fraction) to the prostatic gland and a simultaneous integrated boost (SiB) of 80 Gy (2 Gy per fraction) to the PTV union which was created based on addition of GTV-PET and GTV-MRI. In C the dose wash presentation of the respective RT plan is shown. In the lower row the dose volume histogram (DVH) of the plan is presented for bladder, rectum and the target structures. Abbreviations: PTV = planning target volume, GTV = gross tumour volume.

that in 19% of the sextants, PET imaging detected PCa with a negative result in mpMRI. Conversely, mpMRI was positive with negative PSMA PET imaging in 13% of sextants [27]. Zamboglou et al. reported an increase in sensitivity up to 0.82 when GTV-union (addition between GTV-PET and GTV-MRI) was considered [29]. The use of GTV-intersection (intersection volume between GTV-MRI and GV-PET) increased the specificity to 99%. Accordingly, Rhee et al. stated that not all lesions in histopathology were positive by both: PSMA PET and mpMRI [30].

Whether mpMRI and PSMA PET offer complementary information in GTV characterization remains unclear. A work from the group in Freiburg showed that in patients with multifocal PCa each lesion with the highest SUV (max and mean) had also the lowest ADC (min and mean) and was always the largest lesion in histology [29]. A similar observation was reported by Domachevsky et al. [94], whereas Rowe et al. [15] and Rhee et al. [31] observed only a moderate, inverse correlation between ADC and SUV values.

Currently, clinical data from the implementation of focal RT approaches guided by combined PSMA PET and mpMRI information are lacking. Zamboglou et al. performed a planning study simulating focal IMRT dose escalation according to two published protocols [95]. The TCP was calculated based on the dose distribution in the registered histological information and the focal dose escalation was guided by PSMA PET, mpMRI or the combination of both. Boosting on combined PSMA PET and mpMRI information resulted in significantly increased TCP values without increased risk for normal tissue toxicity in most of the plans.

3.2.4. PET-tracers other than PSMA-ligands

The role of ^{11}C and ^{18}F choline PETCT in the diagnosis of primary PCa is controversially discussed as some studies have shown a low sensitivity for detection of primary PCa, whereas other studies reported a higher sensitivity [96–98]. In a planning study Chang et al. compared mpMRI with [^{11}C] choline-PET/CT for GTV-delineation based on histology reference and postulated a superiority of choline PET/CT [99]. However, more recent data showed that ^{11}C choline PET/CT failed to distinguish between PCa and non-PCa tissue in the prostate [100,101]. Especially benign lesions in the prostate (e.g. BPH nodules, inflammatory lesions) can yield high Choline uptake [102]. A study by Hoffmann et al. compared ^{68}Ga-PSMA-11 PSMA PET/CT with ^{18}F choline PETCT using biopsies as the reference and reported higher sensitivity and specificity for PSMA PET in discrimination of Gleason 7a and 7b tumours [88].

Another potential target receptor for PET-based imaging in patients with primary PCa is the gastrin releasing peptide receptor which can be targeted by ^{68}Ga-labeled antagonists [9,103] and a first in human study demonstrated a sensitivity of 0.88 and a specificity of 0.81 for PCa detection with prostatectomy as reference [103]. A recently published study by Jambor et al. compared ^{18}F- anti-1-amino-3-18F-fluorocyclobutane-1-carboxylic acid (FACBC) PET with mpMRI in detection of primary PCa based on histology reference after operation. The authors stated that ^{18}F-FACBC imaging significantly correlated with Gleason score but failed to outperform mpMRI [104].

4. Discussion

Initial staging of patients with primary PCa has a major impact on further RT procedures and may lead either to treatment intensification (e.g. extended RT fields to the pelvic lymph nodes or to oligometastases, initiation of ADT) or to change of the entire treatment setting (from curative to palliative treatment concept). Likewise, imaging should offer high sensitivity as well as high specificity in order to avoid under- or overtreatment. In regard to bone metastases PSMA PET seems to offer currently the best results in terms of cost effectiveness and diagnostic performance. Notably, current literature on the role of PSMA PET/CT in diagnosis of bone metastases lacks histopathological

reference.

For lymph node staging in patients with primary PCa MR lymphangiography using nanoparticels led to remarkably high sensitivities (> 0.9) [105]. Although PSMA PET has higher sensitivities in detection of lymph node metastases compared to conventional imaging, microscopic disease or affected small volume lymph nodes are potentially missed by PET imaging and thus a negative finding in PSMA PET is not able to rule out metastatic spread within lymph nodes [106]. Furthermore, the study of Thalgott et al. stated that the MSKCC nomogram had a higher concordance with the nodal status in histology than PSMA PET/MRI findings [93]. In our opinion, the use of PSMA PET/CT or mpMRI should therefore not result in an omission of nomogram triggered RT volumes. However, the usage of modern image techniques may enable a directed RT dose escalation to the positive regions or areas (Fig. 1). A current trial (MAGNIFY, NCT03223064, clinicaltrials.org) is recruiting patients in order to compare the accuracy of lymph node staging between ^{68}Ga-PSMA PET and MR lymphangiography with Ferumoxtran-10.

In general both mpMRI and PSMA PET/CT offer acceptable performance for intraprostatic GTV detection and delineation. However, these imaging techniques seem to deliver complementary information as the sensitivity increases when both mpMRI and PSMA PET were combined. Furthermore, IMRT dose escalation on multimodal defined GTVs seems to be feasible and reached the highest TCP values without increase in toxicity. Future studies should identify those patient populations in which a combined use of PSMA PET and mpMRI adds clinical value. In the meanwhile, the combined use of PSMA PET and mpMRI for GTV-delineation is a potential solution to ensure the best therapeutic ratio. It should be mentioned that bowel and bladder motion may lead to a movement of the prostate between acquisitions of different imaging modalities. Therefore, exact co-registration of MRI with PET/CT image data is difficult, which can cause a mismatch of the delineated GTVs. Hybrid PET/MRI systems offer a simultaneous acquisition of the image data and likewise account for this issue.

Several studies reported on interobserver variabilities when intraprostatic GTV was delineated based on mpMRI demonstrating the need for contouring guidelines. CADs may also help to solve this problem but are yet not implemented in clinical routine. For PSMA PET several semiautomatic approaches for GTV-delineation based on SUVmax values (30–50%) within the prostate have been proposed and to the best of our knowledge no CAD for PSMA PET GTV-delineation is available. Future studies should address more deeply on how to contour the intraprostatic GTV based on the currently available imaging modalities.

There is growing evidence that features extracted from mpMRI or PSMA PET/CT may correlate with the biological properties of the intraprostatic GTV. It remains unclear if the combined use may improve GTV characterization. Additionally, there are still no conclusive data on which histopathological parameters should be used to define the tumour aggressiveness. Two studies hypothesized that outcome for patients with primary PCa may be related mainly to the volume and Gleason score of the largest cancer in the prostate [107,108]. It should be mentioned that the lesion with the highest Gleason score may not always be the most relevant for prognosis. Haffner et al. depicted that even a Gleason 6 (3 + 3) lesion may be eventually lethal [109] and De-Colle et al. could show that the ex-vivo yH2AX radiosensitivity of PCa probes is not correlating with the Gleason score, the prostate specific antigen (PSA) serum levels and the tumour stage [110]. Thus, we believe that further research is warranted to improve GTV characterization. Connecting imaging data features with features (e.g. genomics or proteomics) from the corresponding tissue may help to account for interpatient tumor heterogeneity and thus help to characterize the intraprostatic GTV in order to improve risk stratification systems. Recent advances in RT delivery systems like the MR-Linac may enable the depiction of longitudinal, biological changes of the tumor biology during RT based on functional MR images [111]. Mapping and

quantifying these changes has the potential to alter the use of adaptive RT planning and to enable more personalized RT approaches for patients with primary PCa.

In conclusion, multimodal imaging using mpMRI and PSMA PET detects the extraprostatic and intraprostatic tumor burden with a high sensitivity and specificity and has a major impact on RT concepts for patients with primary PCa. It should be mentioned that PSMA PET and mpMRI may offer complementary information for intraprostatic GTV delineation. Furthermore, only moderate interobserver agreement was reported for MRI-based intraprostatic GTV delineation and the implementation of CADs to increase its robustness has not reached the clinical routine yet. Further research is warranted to answer whether multimodal imaging is able to visualize functional and biological processes related to PCa pathophysiology and radiation resistance.

Conflicts of Interest

None.

Appendix A. Supplementary material

Supplementary data to this article can be found online at https://doi.org/10.1016/j.phro.2018.10.001.

References

[1] Mottet N, Bellmunt J, Bolla M, Briers E, Cumberbatch MG, De Santis M, et al. EAU-ESTRO-SIOG Guidelines on prostate cancer. Part 1: screening, diagnosis, and local treatment with curative intent. European Urology 2017;71:618–29.

[2] Martinez AA, Gonzalez J, Ye H, Ghilezan M, Shetty S, Kernen K, et al. Dose escalation improves cancer-related events at 10 years for intermediate- and high-risk prostate cancer patients treated with hypofractionated high-dose-rate boost and external beam radiotherapy. Int J Radiat Oncol Biol Phys 2011;79:363–70.

[3] Zelefsky MJ, Yamada Y, Fuks Z, Zhang Z, Hunt M, Cahlon O, et al. Long-term results of conformal radiotherapy for prostate cancer: impact of dose escalation on biochemical tumor control and distant metastases-free survival outcomes. Int J Radiat Oncol Biol Phys 2008;71:1028–33.

[4] Kishan AU, Cook RR, Ciezki JP, Ross AE, Pomerantz MM, Nguyen PL, et al. Radical prostatectomy, external beam radiotherapy, or external beam radiotherapy with brachytherapy boost and disease progression and mortality in patients with gleason score 9–10 prostate cancer. JAMA 2018;319:896–905.

[5] Viani GA, Stefano EJ, Afonso SL. Higher-than-conventional radiation doses in localized prostate cancer treatment: a meta-analysis of randomized, controlled trials. Int J Radiat Oncol Biol Phys 2009;74:1405–18.

[6] Bauman G, Haider M, Van der Heide UA, Menard C. Boosting imaging defined dominant prostatic tumors: a systematic review. Radiother Oncol 2013;107:274–81.

[7] Eiber M, Weirich G, Holzapfel K, Souvatzoglou M, Haller B, Rauscher I, et al. Simultaneous (68)Ga-PSMA HBED-CC PET/MRI improves the localization of primary prostate cancer. Eur Urol 2016;70:829–36.

[8] Zamboglou C, Schiller F, Fechter T, Wieser G, Jilg CA, Chirindel A, et al. (68)Ga-HBED-CC-PSMA PET/CT versus histopathology in primary localized prostate cancer: a voxel-wise comparison. Theranostics 2016;6:1619–28.

[9] Wieser G, Mansi R, Grosu AL, Schultze-Seemann W, Dumont-Walter RA, Meyer PT, et al. Positron emission tomography (PET) imaging of prostate cancer with a gastrin releasing peptide receptor antagonist-from mice to men. Theranostics 2014;4:412–9.

[10] Zamboglou C, Drendel V, Jilg CA, Rischke HC, Beck TI, Schultze-Seemann W, et al. Comparison of 68Ga-HBED-CC PSMA-PET/CT and multiparametric MRI for gross tumour volume detection in patients with primary prostate cancer based on slice by slice comparison with histopathology. Theranostics 2017;7:228–37.

[11] D'Amico AV, Whittington R, Malkowicz SB, Schultz D, Blank K, Broderick GA, et al. Biochemical outcome after radical prostatectomy, external beam radiation therapy, or interstitial radiation therapy for clinically localized prostate cancer. JAMA 1998;280:969–74.

[12] Williams SG, Duchesne GM, Gogna NK, Millar JL, Pickles T, Pratt GR, et al. An international multicenter study evaluating the impact of an alternative biochemical failure definition on the judgment of prostate cancer risk. Int J Radiat Oncol Biol Phys 2006;65:351–7.

[13] Donati OF, Afaq A, Vargas HA, Mazaheri Y, Zheng JT, Moskowitz CS, et al. Prostate MRI: Evaluating Tumor Volume and Apparent Diffusion Coefficient as Surrogate Biomarkers for Predicting Tumor Gleason Score. Clinical Cancer Research 2014;20:3705–11.

[14] Stoyanova R, Takhar M, Tschudi Y, Ford JC, Solorzano G, Erho N, et al. Prostate cancer radiomics and the promise of radiogenomics. Transl Cancer Res 2016;5:432–47.

[15] Rowe SP, Gage KL, Faraj SF, Macura KJ, Cornish TC, Gonzalez-Roibon N, et al. 18F-DCFBC PET/CT for PSMA-Based Detection and Characterization of Primary Prostate Cancer. J Nucl Med 2015;56:1003–10.

[16] Pasquier D, Henni AH, Escande A, Tresch E, Reynaert N, Colot O, et al. Diffusion weighted MRI as an early predictor of tumor response to hypofractionated stereotactic boost for prostate cancer. Scientific Reports 2018;8..

[17] Boutros PC, Fraser M, Harding NJ, de Borja R, Trudel D, Lalonde E, et al. Spatial genomic heterogeneity within localized, multifocal prostate cancer. Nature Genetics 2015;47:736.

[18] Hovels AM, Heesakkers RAM, Adang EM, Jager GJ, Strum S, Hoogeveen YL, et al. The diagnostic accuracy of CT and MRI in the staging of pelvic lymph nodes in patients with prostate cancer: a meta-analysis. Clin Radiol 2008;63:387–95.

[19] Vallini V, Ortori S, Boraschi P, Manassero F, Gabelloni M, Faggioni L, et al. Staging of pelvic lymph nodes in patients with prostate cancer: Usefulness of multiple b value SE-EPI diffusion-weighted imaging on a 3.0 T MR system. Eur J Radiol Open 2016;3:16–21.

[20] Harisinghani MG, Barentsz J, Hahn PF, Deserno WM, Tabatabaei S, van de Kaa CH, et al. Noninvasive detection of clinically occult lymph-node metastases in prostate cancer. New Engl J Med 2003;348:2491–5.

[21] Woo S, Suh CH, Kim SY, Cho JY, Kim SH. Diagnostic Performance of Magnetic Resonance Imaging for the Detection of Bone Metastasis in Prostate Cancer: A Systematic Review and Meta-analysis. Eur Urol 2018;73:81–91.

[22] Lecouvet FE, Geukens D, Stainier A, Jamar F, Jamart J, d'Othee BJ, et al. Magnetic resonance imaging of the axial skeleton for detecting bone metastases in patients with high-risk prostate cancer: Diagnostic and cost-effectiveness and comparison with current detection strategies. J Clin Oncol 2007;25:3281–7.

[23] Kinoshita Y, Kuratsukuri K, Landas S, Imaida K, Rovito PM, Wang CY, et al. Expression of prostate-specific membrane antigen in normal and malignant human tissues. World J Surg 2006;30:628–36.

[24] Bostwick DG, Pacelli A, Blute M, Roche P, Murphy GP. Prostate specific membrane antigen expression in prostatic intraepithelial neoplasia and adenocarcinoma – a study of 184 cases. Cancer 1998;82:2256–61.

[25] Mannweiler S, Amersdorfer P, Trajanoski S, Terrett JA, King D, Mehes G. Heterogeneity of Prostate-Specific Membrane Antigen (PSMA) Expression in Prostate Carcinoma with Distant Metastasis. Pathol Oncol Res 2009;15:167–72.

[26] Fendler WP, Schmidt DF, Wenter V, Thierfelder KM, Zach C, Stief C, et al. 68Ga-PSMA PET/CT Detects the Location and Extent of Primary Prostate Cancer. J Nucl Med 2016;57:1720–5.

[27] Eiber M, Weirich G, Holzapfel K, Souvatzoglou M, Haller B, Rauscher I, et al. Simultaneous Ga-PSMA HBED-CC PET/MRI Improves the Localization of Primary Prostate Cancer. Eur Urol 2016.

[28] Rahbar K, Weckesser M, Huss S, Semjonow A, Breyholz HJ, Schrader AJ, et al. Correlation of intraprostatic tumor extent with 68-Ga-PSMA distribution in patients with prostate cancer. J Nucl Med 2016.

[29] Zamboglou C, Drendel V, Jilg CA, Rischke HC, Beck TI, Schultze-Seemann W, et al. Comparison of (68)Ga-HBED-CC PSMA-PET/CT and multiparametric MRI for gross tumour volume detection in patients with primary prostate cancer based on slice by slice comparison with histopathology. Theranostics 2017;7:228–37.

[30] Rhee H, Thomas P, Shepherd B, Gustafson S, Vela I, Russell PJ, et al. Prostate Specific Membrane Antigen Positron Emission Tomography May Improve the Diagnostic Accuracy of Multiparametric Magnetic Resonance Imaging in Localized Prostate Cancer. J Urol 2016;196:1261–6.

[31] Kesch C, Vinsensia M, Radtke JP, Schlemmer HP, Heller M, Ellert E, et al. Intraindividual Comparison of F-18-PSMA-1007 PET/CT, Multiparametric MRI, and radical prostatectomy specimens in patients with primary prostate cancer: a retrospective proof-of-concept study. J Nucl Med 2017;58:1805–10.

[32] Zschaeck S, Lohaus F, Beck M, Habl G, Kroeze S, Zamboglou C, et al. PSMA-PET based radiotherapy: a review of initial experiences, survey on current practice and future perspectives. Radiat Oncol 2018;13.

[33] Gorin MA, Rowe SP, Patel HD, Vidal I, Mana-Ay M, Javadi MS, et al. Prostate specific membrane antigen targeted (18)F-DCFPyL positron emission tomography/computerized tomography for the preoperative staging of high risk prostate cancer: results of a prospective, phase II. Single center study. J Urol 2018;199:126–32.

[34] Maurer T, Gschwend JE, Rauscher I, Souvatzoglou M, Haller B, Weirich G, et al. Diagnostic efficacy of (68)Gallium-PSMA positron emission tomography compared to conventional imaging for lymph node staging of 130 consecutive patients with intermediate to high risk prostate cancer. J Urol 2016;195:1436–42.

[35] van Leeuwen PJ, Emmett L, Ho B, Delprado W, Ting F, Nguyen Q, et al. Prospective evaluation of 68Gallium-prostate-specific membrane antigen positron emission tomography/computed tomography for preoperative lymph node staging in prostate cancer. BJU Int 2017;119:209–15.

[36] Obek C, Doganca T, Demirci E, Ocak M, Kural AR, Yildirim A, et al. The accuracy of (68)Ga-PSMA PET/CT in primary lymph node staging in high-risk prostate cancer. Eur J Nucl Med Mol Imaging 2017;44:1806–12.

[37] Mix M, Reichel K, Stoykow C, Bartholoma M, Drendel V, Gourni E, et al. Performance of (111)In-labelled PSMA ligand in patients with nodal metastatic prostate cancer: correlation between tracer uptake and histopathology from lymphadenectomy. Eur J Nucl Med Mol Imaging 2018.

[38] Rischpler C, Beck TI, Okamoto S, Schlitter AM, Knorr K, Schwaiger M, et al. (68)Ga-PSMA-HBED-CC uptake in cervical, coeliac and sacral ganglia as an important pitfall in prostate cancer PET imaging. J Nucl Med 2018.

[39] Pyka T, Okamoto S, Dahlbender M, Tauber R, Retz M, Heck M, et al. Comparison of bone scintigraphy and (68)Ga-PSMA PET for skeletal staging in prostate cancer. Eur J Nucl Med Mol Imaging 2016;43:2114–21.

[40] Thomas L, Balmus C, Ahmadzadehfar H, Essler M, Strunk H, Bundschuh RA. Assessment of bone metastases in patients with prostate cancer—a comparison between Tc-99m-bone-scintigraphy and [Ga-68]Ga-PSMA PET/CT.

Pharmaceuticals 2017;10.

[41] Sheikhbahaei S, Afshar-Oromieh A, Eiber M, Solnes LB, Javadi MS, Ross AE, et al. Pearls and pitfalls in clinical interpretation of prostate-specific membrane antigen (PSMA)-targeted PET imaging. Eur J Nucl Med Mol Imaging 2017;44:2117–36.

[42] Roach PJ, Francis R, Emmett L, Hsiao E, Kneebone A, Hruby G, et al. The impact of (68)Ga-PSMA PET/CT on management intent in prostate cancer: results of an australian prospective multicenter study. J Nucl Med 2018;59:82–8.

[43] Dewes S, Schiller K, Sauter K, Eiber M, Maurer T, Schwaiger M, et al. Integration of (68)Ga-PSMA-PET imaging in planning of primary definitive radiotherapy in prostate cancer: a retrospective study. Radiat Oncol 2016;11:73.

[44] Schiller K, Devecka M, Maurer T, Eiber M, Gschwend J, Schwaiger M, et al. Impact of (68)Ga-PSMA-PET imaging on target volume definition and guidelines in radiation oncology – a patterns of failure analysis in patients with primary diagnosis of prostate cancer. Radiat Oncol 2018;13:36.

[45] Shreve PD, Grossman HB, Gross MD, Wahl RL. Metastatic prostate cancer: initial findings of PET with 2-deoxy-2-[F-18]fluoro-D-glucose. Radiology 1996;199:751–6.

[46] Ghanem N, Uhl M, Brink I, Schafer O, Kelly T, Moser E, et al. Diagnostic value of MRI in comparison to scintigraphy, PET, MS-CT and PET/CT for the detection of metastases of bone. Eur J Radiol 2005;55:41–55.

[47] Schwarzenbock S, Souvatzoglou M, Krause BJ. Choline PET and PET/CT in primary diagnosis and staging of prostate cancer. Theranostics 2012;2:318–30.

[48] Evangelista L, Guttilla A, Zattoni F, Muzzio PC, Zattoni F. Utility of choline positron emission tomography/computed tomography for lymph node involvement identification in intermediate- to high-risk prostate cancer: a systematic literature review and meta-analysis. Eur Urol 2013;63:1040–8.

[49] Selnaes KM, Kruger-Stokke B, Elschot M, Willoch F, Storkersen O, Sandsmark E, et al. (18)F-Fluciclovine PET/MRI for preoperative lymph node staging in high-risk prostate cancer patients. Eur Radiol 2018.

[50] Mosavi F, Johansson S, Sandberg DT, Turesson I, Sorensen J, Ahlstrom H. Whole-body diffusion-weighted MRI compared with (18)F-NaF PET/CT for detection of bone metastases in patients with high-risk prostate carcinoma. AJR Am J Roentgenol 2012;199:1114–20.

[51] Chen S, Cheung SK, Wong KN, Wong KK, Ho CL. 68Ga-DOTATOC and 68Ga-PSMA PET/CT unmasked a case of prostate cancer with neuroendocrine differentiation. Clin Nucl Med 2016;41:959–60.

[52] de Rooij M, Hamoen EH, Futterer JJ, Barentsz JO. Rovers MM. Accuracy of multiparametric MRI for prostate cancer detection: a meta-analysis. AJR Am J Roentgenol 2014;202:343–51.

[53] Woo S, Suh CH, Kim SY, Cho JY, Kim SH. Diagnostic performance of prostate imaging reporting and data system version 2 for detection of prostate cancer: a systematic review and diagnostic meta-analysis. Eur Urol 2017;72:177–88.

[54] Schmuecking M, Boltze C, Geyer H, Salz H, Schilling B, Wendt TG, et al. Dynamic MRI and CAD vs. Choline MRS: Where is the detection level for a lesion characterisation in prostate cancer? International Journal of Radiation Biology 2009;85:814–24.

[55] Bonekamp D, Jacobs MA, El-Khouli R, Stoianovici D, Macura KJ. Advancements in MR imaging of the prostate: from diagnosis to interventions. Radiographics 2011;31:677–703.

[56] Barrett T, Gill AB, Kataoka MY, Priest AN, Joubert I, McLean MA, et al. DCE and DW MRI in monitoring response to androgen deprivation therapy in patients with prostate cancer: A feasibility study. Magnet Reson Med 2012;67:778–85.

[57] Ruprecht O, Weisser P, Bodelle B, Ackermann H. Vogl TJ. MRI of the prostate: Interobserver agreement compared with histopathologic outcome after radical prostatectomy. Eur J Radiol 2012;81:456–60.

[58] Steenbergen P, Haustermans K, Lerut E, Oyen R, De Weyer L, Van den Bergh L, et al. Prostate tumor delineation using multiparametric magnetic resonance imaging: Inter-observer variability and pathology validation. Radiother Oncol 2015;115:186–90.

[59] van Schie MA, Dinh CV, Houdt PJV, Pos FJ, Heijmink S, Kerkmeijer LGW, et al. Contouring of prostate tumors on multiparametric MRI: Evaluation of clinical delineations in a multicenter radiotherapy trial. Radiother Oncol 2018.

[60] Rischke HC, Nestle U, Fechter T, Doll C, Volegova-Neher N, Henne K, et al. 3 Tesla multiparametric MRI for GTV-definition of dominant intraprostatic lesions in patients with prostate cancer—an interobserver variability study. Radiat Oncol 2013;8:183.

[61] Weinreb JC, Barentsz JO, Choyke PL, Cornud F, Haider MA, Macura KJ, et al. PI-RADS prostate imaging – reporting and data system: 2015, Version 2. Eur Urol 2016;69:16–40.

[62] Venderink W, van Luijtelaar A, Bomers JGR, van der Leest M, De Kaa CHV, Barentsz JO, et al. Results of targeted biopsy in men with magnetic resonance imaging lesions classified equivocal, likely or highly likely to be clinically significant prostate cancer. Eur Urol 2018;73:353–60.

[63] Thai JN, Narayanan HA, George AK, Siddiqui MM, Shah P, Mertan FV, et al. Validation of PI-RADS version 2 in transition zone lesions for the detection of prostate cancer. Radiology 2018;170425.

[64] Seo JW, Shin SJ, Taik OhY, Jung DC, Cho NH, Choi YD, et al. PI-RADS version 2: detection of clinically significant cancer in patients with biopsy gleason score 6 prostate cancer. AJR Am J Roentgenol 2017;209:W1–9.

[65] Dinh CV, Steenbergen P, Ghobadi G, Heijmink SW, Pos FJ, Haustermans K, et al. Magnetic resonance imaging for prostate cancer radiotherapy. Phys Med 2016;32:446–51.

[66] Viswanath SE, Bloch NB, Chappelow JC, Toth R, Rofsky NM, Genega EM, et al. Central gland and peripheral zone prostate tumors have significantly different quantitative imaging signatures on 3 tesla endorectal, in vivo T2-weighted MR imagery. Journal of Magnetic Resonance Imaging 2012;36:213–24.

[67] Tsehay YK, Lay NS, Roth HR, Wang XS, Kwak JT, Turkbey BI, et al. Convolutional neural network based deep-learning architecture for prostate cancer detection on multiparametric magnetic resonance images. Medical Imaging 2017: Computer-Aided Diagnosis 2017:10134.

[68] Liu SF, Zheng HX, Feng YS, Li W. Prostate cancer diagnosis using deep learning with 3D multiparametric MRI. Medical Imaging 2017: Computer-Aided Diagnosis 2017:10134.

[69] Algohary A, Viswanath S, Shiradkar R, Ghose S, Pahwa S, Moses D, et al. Radiomic features on MRI enable risk categorization of prostate cancer patients on active surveillance: preliminary findings. J Magn Reson Imaging 2018.

[70] Wang XG, Yang W, Weinreb J, Han J, Li QB, Kong XC, et al. Searching for prostate cancer by fully automated magnetic resonance imaging classification: deep learning versus non-deep learning. Sci Rep 2017;7..

[71] Arrayeh E, Westphalen AC, Kurhanewicz J, Roach M, Jung AJ, Carroll PR, et al. Does local recurrence of prostate cancer after radiation therapy occur at the site of primary tumor? Results of a longitudinal MRI and MRSI study. Int J Radiat Oncol Biol Phys 2012;82:E787–93.

[72] Pucar D, Hricak H, Shukla-Dave A, Kuroiwa K, Drobnjak M, Eastham J, et al. Clinically significant prostate cancer local recurrence after radiation therapy occurs at the site of primary tumor: magnetic resonance imaging and step-section pathology evidence. Int J Radiat Oncol Biol Phys 2007;69:62–9.

[73] Mendez LC, Ravi A, Chung H, Tseng CL, Wronski M, Paudel N, et al. Pattern of relapse and dose received by the recurrent intraprostatic nodule in low- to intermediate-risk prostate cancer treated with single fraction 19 Gy high dose-rate brachytherapy. Brachytherapy 2017.

[74] Quivrin M, Loffroy R, Cormier L, Mazoyer F, Bertaut A, Chambade D, et al. Multiparametric MRI and post implant CT-based dosimetry after prostate brachytherapy with iodine seeds: the higher the dose to the dominant index lesion, the lower the PSA bounce. Radiother Oncol 2015;117:258–61.

[75] Zamboglou C, Klein CM, Thomann B, Fassbender TF, Rischke HC, Kirste S, et al. The dose distribution in dominant intraprostatic tumour lesions defined by multiparametric MRI and PSMA PET/CT correlates with the outcome in patients treated with primary radiation therapy for prostate cancer. Radiat Oncol 2018;13:65.

[76] Gibbs P, Liney GP, Pickles MD, Zelhof B, Rodrigues G. Turnbull LW. correlation of ADC and T2 measurements with cell density in prostate cancer at 3.0 Tesla. Investigative Radiology 2009;44:572–6.

[77] Casares-Magaz O, van der Heide UA, Rorvik J, Steenbergen P, Muren LP. A tumour control probability model for radiotherapy of prostate cancer using magnetic resonance imaging-based apparent diffusion coefficient maps. Radiother Oncol 2016;119:111–6.

[78] Joseph T, McKenna DA, Westphalen AC, Coakley FV, Zhao SJ, Lu Y, et al. Pretreatment Endorectal Magnetic Resonance Imaging and Magnetic Resonance Spectroscopic Imaging Features of Prostate Cancer as Predictors of Response to External Beam Radiotherapy. Int J Radiat Oncol Biol Phys 2009;73:665–71.

[79] McKenna DA, Coakley FV, Westphalen AC, Zhao S, Lu Y, Webb EM, et al. Prostate cancer: role of pretreatment MR in predicting outcome after external-beam radiation therapy–initial experience. Radiology 2008;247:141–6.

[80] Gnep K, Fargeas A, Gutierrez-Carvajal RE, Commandeur F, Mathieu R, Ospina JD, et al. Haralick textural features on T2 -weighted MRI are associated with biochemical recurrence following radiotherapy for peripheral zone prostate cancer. J Magn Reson Imaging 2017;45:103–17.

[81] Song I, Kim CK, Park BK, Park W. Assessment of response to radiotherapy for prostate cancer: value of diffusion-weighted MRI at 3 T. Am J Roentgenol 2010;194:W477–82.

[82] Gomez-Iturriaga A, Casquero F, Urresola A, Ezquerro A, Lopez JI, Espinosa JM, et al. Dose escalation to dominant intraprostatic lesions with MRI-transrectal ultrasound fusion High-Dose-Rate prostate brachytherapy. Prospective phase II trial. Radiother Oncol 2016;119:91–6.

[83] Monninkhof EM, van Loon JWL, van Vulpen M, Kerkmeijer LGW, Pos FJ, Haustermans K, et al. Standard whole prostate gland radiotherapy with and without lesion boost in prostate cancer: toxicity in the FLAME randomized controlled trial. Radiother Oncol 2018;127:74–80.

[84] Lopci E, Saita A, Lazzeri M, Lughezzani G, Colombo P, Buffi NM, et al. Ga-68-PSMA positron emission tomography/computerized tomography for primary diagnosis of prostate cancer in men with contraindications to or negative multiparametric magnetic resonance imaging: a prospective observational study. J Urol 2018;200:95–103.

[85] Giesel FL, Sterzing F, Schlemmer HP, Holland-Letz T, Mier W, Rius M, et al. Intra-individual comparison of (68)Ga-PSMA-11-PET/CT and multi-parametric MR for imaging of primary prostate cancer. Eur J Nucl Med Mol Imaging 2016;43:1400–6.

[86] Thomas L, Kantz S, Hung A, Monaco D, Gaertner FC, Essler M, et al. (68)Ga-PSMA-PET/CT imaging of localized primary prostate cancer patients for intensity modulated radiation therapy treatment planning with integrated boost. Eur J Nucl Med Mol Imaging 2018;45:1170–8.

[87] Bravaccini S, Puccetti M, Bocchini M, Ravaioli S, Celli M, Scarpi E, et al. PSMA expression: a potential ally for the pathologist in prostate cancer diagnosis. Sci Rep 2018;8:4254.

[88] Hoffmann MA, Miederer M, Wieler HJ, Ruf C, Jakobs FM, Schreckenberger M. Diagnostic performance of (68)Gallium-PSMA-11 PET/CT to detect significant prostate cancer and comparison with (18)FEC PET/CT. Oncotarget 2017;8:111073–83.

[89] Lips IM, van der Heide UA, Haustermans K, van Lin EN, Pos F, Franken SP, et al. Single blind randomized phase III trial to investigate the benefit of a focal lesion ablative microboost in prostate cancer (FLAME-trial): study protocol for a randomized controlled trial. Trials 2011;12:255.

[90] Zamboglou C, Sachpazidis I, Koubar K, Drendel V, Wiehle R, Kirste S, et al. Evaluation of intensity modulated radiation therapy dose painting for localized prostate cancer using (68)Ga-HBED-CC PSMA-PET/CT: A planning study based on histopathology reference. Radiother Oncol 2017;123:472–7.

[91] Zamboglou C, Wieser G, Hennies S, Rempel I, Kirste S, Soschynski M, et al. MRI versus (68)Ga-PSMA PET/CT for gross tumour volume delineation in radiation treatment planning of primary prostate cancer. Eur J Nucl Med Mol Imaging 2016;43:889–97.

[92] Tulsyan S, Das CJ, Tripathi M, Seth A, Kumar R, Bal C. Comparison of 68Ga-PSMA PET/CT and multiparametric MRI for staging of high-risk prostate cancer68Ga-PSMA PET and MRI in prostate cancer. Nucl Med Commun 2017;38:1094–102.

[93] Thalgott M, Duwel C, Rauscher I, Heck MM, Haller B, Gafita A, et al. One-stop shop whole-body (68)Ga-PSMA-11 PET/MRI compared to clinical Nomograms for preoperative T- and N-Staging of High-Risk Prostate Cancer. J Nucl Med 2018.

[94] Domachevsky L, Goldberg N, Bernstine H, Nidam M, Groshar D. Quantitative characterisation of clinically significant intra-prostatic cancer by prostate-specific membrane antigen (PSMA) expression and cell density on PSMA-11. Eur Radiol 2018.

[95] Zamboglou C, Thomann B, Koubar K, Bronsert P, Krauss T, Rischke HC, et al. Focal dose escalation for prostate cancer using (68)Ga-HBED-CC PSMA PET/CT and MRI: a planning study based on histology reference. Radiat Oncol 2018;13:81.

[96] Chang JH, Joon DL, Lee ST, Gong SJ, Scott AM, Davis ID, et al. Histopathological correlation of (11)C-choline PET scans for target volume definition in radical prostate radiotherapy. Radiother Oncol 2011;99:187–92.

[97] Farsad M, Schiavina R, Castellucci P, Nanni C, Corti B, Martorana G, et al. Detection and localization of prostate cancer: correlation of (11)C-choline PET/CT with histopathologic step-section analysis. J Nucl Med 2005;46:1642–9.

[98] Jadvar H. Prostate cancer: PET with 18F-FDG, 18F- or 11C-acetate, and 18F- or 11C-choline. J Nucl Med 2011;52:81–9.

[99] Chang JH, Joon DL, Lee ST, Gong SJ, Anderson NJ, Scott AM, et al. Intensity Modulated Radiation Therapy Dose Painting for Localized Prostate Cancer Using C-11-choline Positron Emission Tomography Scans. Int J Radiat Oncol Biol Phys 2012;83:E691–6.

[100] Bundschuh RA, Wendl CM, Weirich G, Eiber M, Souvatzoglou M, Treiber U, et al. Tumour volume delineation in prostate cancer assessed by [C-11]choline PET/CT: validation with surgical specimens. Eur J Nucl Med Mol Imaging 2013;40:824–31.

[101] Grosu AL, Weirich G, Wendl C, Prokic V, Kirste S, Geinitz H, et al. 11C-Choline PET/pathology image coregistration in primary localized prostate cancer. Eur J Nucl Med Mol Imaging 2014;41:2242–8.

[102] Souvatzoglou M, Weirich G, Schwarzenboeck S, Maurer T, Schuster T, Bundschuh RA, et al. The sensitivity of [11C]choline PET/CT to localize prostate cancer depends on the tumor configuration. Clin Cancer Res 2011;17:3751–9.

[103] Kahkonen E, Jambor I, Kemppainen J, Lehtio K, Gronroos TJ, Kuisma A, et al. In vivo imaging of prostate cancer using [68Ga]-labeled bombesin analog BAY86-7548. Clin Cancer Res 2013;19:5434–43.

[104] Jambor I, Kuisma A, Kahkonen E, Kemppainen J, Merisaari H, Eskola O, et al. Prospective evaluation of (18)F-FACBC PET/CT and PET/MRI versus multiparametric MRI in intermediate- to high-risk prostate cancer patients (FLUCIPRO trial). Eur J Nucl Med Mol Imaging 2018;45:355–64.

[105] Daldrup-Link HE. Ten things you might not know about iron oxide nanoparticles. Radiology 2017;284:616–29.

[106] Jilg CA, Drendel V, Rischke HC, Beck T, Vach W, Schaal K, et al. Diagnostic Accuracy of Ga-68-HBED-CC-PSMA-Ligand-PET/CT before salvage lymph node dissection for recurrent prostate cancer. Theranostics 2017;7:1770–80.

[107] Stamey TA, Mcneal JE, Freiha FS, Redwine E. Morphometric and clinical-studies on 68 consecutive radical prostatectomies. J Urol 1988;139:1235–41.

[108] McNeal JE, Villers AA, Redwine EA, Freiha FS, Stamey TA. Histologic differentiation, cancer volume, and pelvic lymph node metastasis in adenocarcinoma of the prostate. Cancer 1990;66:1225–33.

[109] Haffner MC, Mosbruger T, Esopi DM, Fedor H, Heaphy CM, Walker DA, et al. Tracking the clonal origin of lethal prostate cancer. J Clin Invest 2013;123:4918–22.

[110] De-Colle C, Yaromina A, Hennenlotter J, Thames H, Mueller AC, Neumann T, et al. Ex vivo gammaH2AX radiation sensitivity assay in prostate cancer: Inter-patient and intra-patient heterogeneity. Radiother Oncol 2017;124:386–94.

[111] Datta A, Aznar MC, Dubec M, Parker GJM, O'Connor JPB. Delivering functional imaging on the MRI-linac: current challenges and potential solutions. Clin Oncol (R Coll Radiol) 2018;30:702–10.

[112] Berger I, Annabattula C, Lewis J, Shetty DV, Kam J, Maclean F, et al. (68)Ga-PSMA PET/CT vs. mpMRI for locoregional prostate cancer staging: correlation with final histopathology. Prostate Cancer Prostatic Dis 2018;21:204–11.